Silicon Radio-Frequency Planar Nanofluidic Channels

Chunrong Song, Jiwei Sun, Yuxi He and Pingshan Wang

Department of Electrical and Computer Engineering, Clemson University, Clemson, SC 29634, USA

Abstract — Ten-nanometer deep planar nanofluidic channels are designed, fabricated and characterized. Silicon microstrip lines are incorporated with the nanofluidic channels to provide broadband radio frequency (RF) measurement capabilities so that materials in the channels can be investigated in a label-free and non-invasive manner. Deionized water in the 10 nm channels is tested to demonstrate the operation of the devices. The techniques are promising to address the electrical sensing and signal transduction issues in current nanochannel efforts. Further work on reliable and repeatable probe contacts and silicon transmission line dispersion properties is needed for quantitative analysis of materials in the channels.

Index Terms — Nanofluidic channel, radio frequency, scattering parameter, transmission line.

I. INTRODUCTION

Nanofluidic channels are of great interest for various novel applications, such as DNA separation, sorting and sequencing [1], water desalination [2], and fluidic electronics development [3]. Nanofluidic channels are also essential for the study of a range of phenomena and processes, including water confinement [4] and electrical double layers [5].

Current nanochannel fabrication techniques include nanolithography [6], nanoglassblowing [7], nanoimprint lithography [8], polysisesquioxane sealing [9], and native oxide etching (NOE) [10]. Among these approaches, NOE has been demonstrated to provide accurate and reliable control of planar nano-trenches with depth down to ~ 1 nm. Nevertheless, current methods for sensing and analyzing materials in nanofluidic channels are limited to optical observations and DC/low-frequency electrical measurements. The former needs transparent channels and fluorescence labeling [9]. The latter is hindered by electrical double layers. Broadband dielectric spectroscopy [11] can overcome these restrictions and complement current methods as demonstrated in various studies, such as DNA analysis [12], molecular structure probing [13], and confined-water-dynamics investigation [14]. In this work, we show that broadband high-frequency measurement capabilities can be incorporated into nanofluidic channels that are formed with the simple NOE techniques.

II. DEVICE DESIGN AND FABRICATION

Figure 1 shows RF nanofluidic channels (light-blue fingers) that are imbedded in the signal trace of a microstrip line, which is formed with silicon wafers. The top wafer forms the ground while the silicon-on-insulator (SOI) wafer forms the signal trace. Uniform electric fields in nanofluidic channels (Fig. 1(b)) and convenient fabrication processes are the main advantages for choosing microstrip line structures. Coplanar Waveguide (CPW) transition sections (50 Ω) are used for ground-signal-ground (GSG) probing.

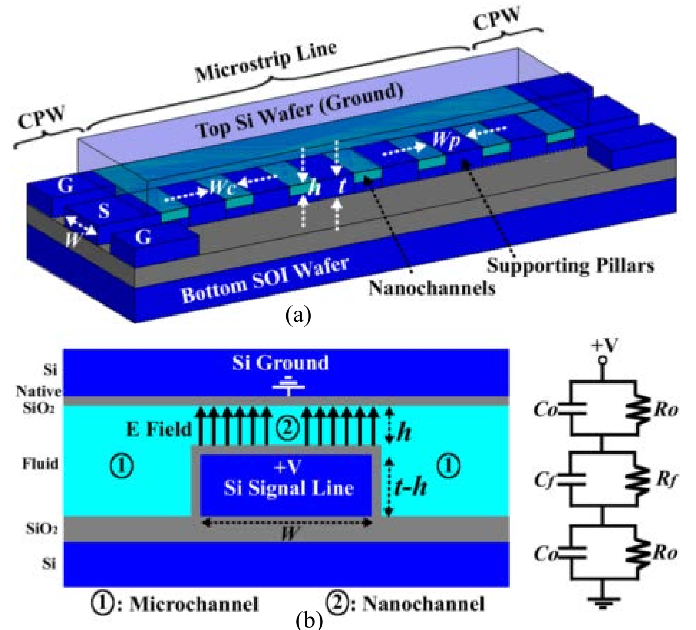

Fig.1. (a) An illustration of the RF nanofluidic channels. Part of the top silicon wafer and water (light-blue) are not drawn to show channel layout. (b) A cross section of an RF nanofluidic channel and an equivalent circuit model of the nanochannel in the transverse direction. Subscripts "*o*" and "*f*" are for native oxide and fluid, respectively. Drawing is not to scale.

A. Design Considerations

To obtain 10 nm fluidic channels in a reliable and controllable manner, trenches with nanometer depth and atomically flat surfaces can be created with silicon (Si) substrates by etching native oxide layers [10]. To reduce Si microstrip-line loss, heavily doped Si substrate with a resistivity of 0.001-0.002 Ω•cm need to be used. Nevertheless, the resistivity is still ~ 3 orders of magnitude higher than that of commonly used metal films, such as Al. Consequently, Si microstrip line length is limited due to high-loss, which prohibits wide use of Si transmission lines despite the fact that polysilicon lines have been used exclusively for local interconnect (~10 µm or shorter) in VLSI technologies.

Impedance mismatch between the microstrip line (characteristic impedance Z_1) and the measurement system (Z_0,

978-1-4673-2141-9/13/$31.00 ©2013 IEEE

50 Ω) is another issue. Microstrip line width W (i.e. channel length in Fig. 1) needs to be controlled for a given channel depth (h) so that mismatch loss, $RL = -20log|(Z_1 - Z_0)/(Z_1 + Z_0)|$ dB, is acceptable. Nevertheless, W cannot be too small since W also affect line loss, $\alpha_c = Rs/(Z_1 \times W)$ Np/m, where Rs is the surface resistance of Si [15]. On the other hand, large channel width Wc is needed so that there are sufficient fluids in the channel to induce measureable scattering parameter changes. But Wc is limited by the requirement $h < 3.6 (Wc \times \gamma / E)^{0.5}$, where γ is surface energy and E is the Young's modulus of silicon substrate [16]. Hence a channel array is needed with supporting pillars between adjacent channels to ensure channel integrity. Consequently, the nanochannels and supporting pillars yield two different microstrip line sections. One has two bonded native oxide layers (~3-4 nm in thickness); the other also includes fluids inside the nanochannel, Fig. 1(b). Consider the above issues, an array of 43 individual channels with h = 10 nm, Wc = 2 μm, and Wp = 5 μm is designed. Advanced Design System simulations are conducted with estimated substrate and water properties. The obtained results show that 300 μm long Si microstrip lines are reasonable for material characterizations.

B. Fabrication Processes

There are three major steps in device fabrication: form signal line and nano-trenches on the bottom SOI wafer, create windows for measurement contacts (GSG) and liquid inlet/outlet on top wafer, and bond wafers.

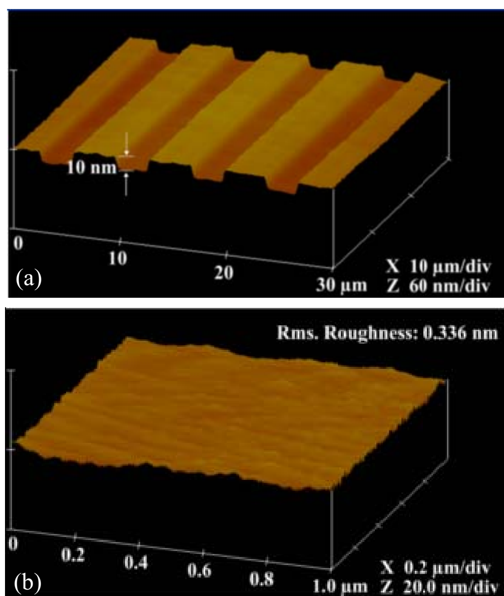

Fig.2. AFM images of 10 nm deep Si nano-trenches. (a) 3-D view. (b) Rms. roughness of 0.336 nm of a trench surface.

Figure 2 shows typical 3-D images of the obtained Si nanotrenches and trench surface roughness on an SOI wafer that has a 25 μm thick N-type Si device layer, a 2 μm thick SiO2 box layer and a 500 μm thick N-type Si handle layer.

Standard deep-reactive-ion-etch (DRIE) is used to etch through the 350 μm thick top Si wafer to form probing windows and liquid inlet/outlet windows. Then Si-Si direct fusion bonding process is used to seal the nanotrenches and obtain 10 nm fluidic channels with an inverted microstrip line, shown in Fig. 3. The integrity of the formed nanochannels is examined through scanning electron microscope (SEM), in Fig. 4, which shows an SEM image of the cross section of a 10 nm channel. Seamless Si-Si bonding interface indicates good wafer bonding and strong bonding strength.

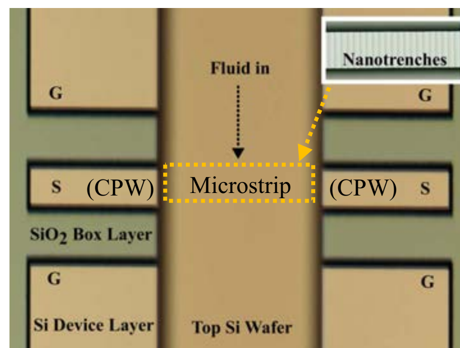

Fig.3. Microscopy image of a final device after bonding the top wafer with the bottom wafer. The inset shows the nano-trench array.

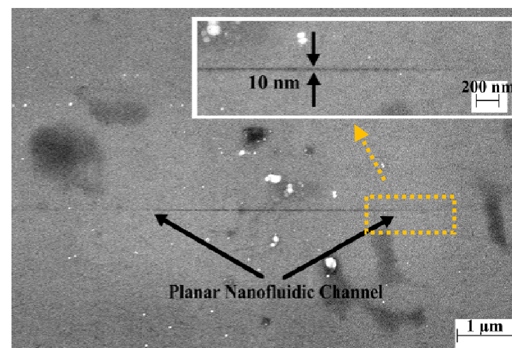

Fig. 4. An SEM cross-section view of a 10 nm Si fluidic channel.

III. MEASUREMENT RESULTS AND DISCUSSIONS

To measure the scattering parameters of the fabricated devices, reasonable electrical contacts between GSG probe tips and silicon GSG contact pads are obtained and verified through DC measurements of contact resistance. Fig. 5 shows the measured magnitudes of S_{11} and S_{21} when the nanofluidic channels are filled with and without deionized water.

When there is no water in the nanochannels, the measured transmission coefficient S_{21} is at a level of around - 40 dB. The introduction of water reduces S_{21} by up to 20 dB due to higher dielectric & conductive losses, and worse match conditions at the CPW to microstrip line transition interfaces. The reflection coefficient S_{11} does not change noticeably owing to high base-level reflection coefficients. Another dummy test device is measured in order to verify the 20 dB change is indeed caused by water inside the nanochannel arrays. The dummy test device is without nanochannels but otherwise identical to the RF nanochannel device. So water cannot appear between the signal trace and ground plane of

978-1-4673-2141-9/13/$31.00 ©2013 IEEE

the inverted microstrip line. No noticeable transmission scattering parameter changes are observed when water is injected into the microfluidic channels even though the absolute S_{21} values are somewhat different from those shown in Fig. 5.

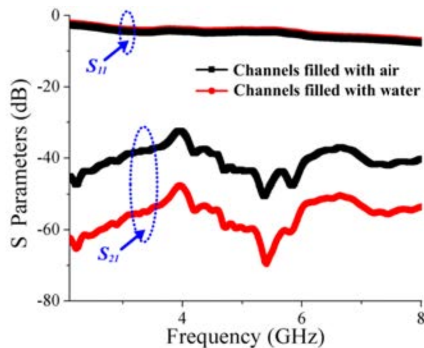

Fig.5. Measured S-Parameters (magnitude) before/after DI water (18 MΩ•cm resistivity) injection.

An additional advantage of our RF nanofluidic channels is convenient electrical control of channel surface charges, for which current techniques are limited to adjusting nanochannel solution PH levels [17], coating nanochannel surface [18], and electrical gating of the channels [19]. Current electrical gating usually require high voltage operations due to relatively deep channels and thick "gate" oxide layers [19], analogous to that of a field effect transistor. High-voltages across the channels could initiate un-intended processes, such as electrolysis that occurs at ~ 1.23V. Therefore, our 10 nm nanochannels and ~ 1 nm level gating oxide thickness lower gating voltages significantly. The simple circuit model in Fig. 1(b) can be used to analyze electrically induced surface charges. Additionally, the channel depth can be further scaled down to ~ 1 nm.

The above results show that the fabricated RF nanofluidic channels can be used for the detection and analysis of fluidic samples from measured (relative) scattering parameter differences. However, a few issues need to be addressed for quantitative characterization of fluids in nanofluidic channels. The first is reliable and repeatable contacts between GSG probe tips and silicon transmission lines. Possible solutions include depositing metal thin films over silicon GSG contact pads. The second is to further understand silicon-based transmission lines, which are more dispersive than metallic lines. The dispersion further complicates the interpretation of the obtained S-parameters, such as that in Fig. 5, and material parameter extractions.

IV. Conclusions

Silicon RF nanofluidic channels are designed, fabricated and tested. Heavily-doped SOI substrates are used to build 10 nm channel arrays, and the channels are incorporated into a silicon microstrip line to provide broadband measurement capabilities. The operation of the device is demonstrated by measuring microstrip line scattering parameters with DI water in the nanofluidic channels. The RF silicon electrodes also enable electrical control and manipulation of channel surface charges. Further work on reliable & repeatable contacts and silicon transmission line dispersion properties is needed for quantitative analysis applications.

Acknowledgement

The work is supported by National Science Foundation (NSF) under Award #2007344. The fabrication is conducted at Cornell NanoScale Science and Technology Facility (CNF) in Cornell University.

References

[1] J. Han, H.G. Craighead, "Separation of long DNA molecules in a microfabricated entropic trap array," *Science*, vol. 288, pp. 1026-1029, 2000.
[2] S.J. Kim, S.H. Ko, K.H. Kang, J. Han, "Direct seawater desalination by ion concentration polarization," *Nat. Nanotechnol.*, vol. 5, pp. 297-301, 2010.
[3] M.A.M. Gijs, "Device physics - Will fluidic electronics take off?," *Nat. Nanotechnol.*, vol. 2, pp. 268-270, 2007.
[4] J.J. Gilijamse, A.J. Lock, H.J. Bakker, "Dynamics of confined water molecules," *Proc Natl Acad Sci U S A*, vol. 102, pp. 3202-3207, 2005.
[5] J.C.T. Eijkel, A. van den Berg, "Nanofluidics: what is it and what can we expect from it?," *Microfluid. Nanofluid.*, vol. 1, pp. 249-267, 2005.
[6] Q.F. Xia, K.J. Morton, R.H. Austin, S.Y. Chou, "Sub-10 nm Self-Enclosed Self-Limited Nanofluidic Channel Arrays," *Nano Letters*, vol. 8, pp. 3830-3833, 2008.
[7] E.A. Strychalski, S.M. Stavis, H.G. Craighead, "Non-planar nanofluidic devices for single molecule analysis fabricated using nanoglassblowing," *Nanotechnology*, vol. 19, pp. 315301-315308, 2008.
[8] H. Cao, Z.N. Yu, J. Wang, J.O. Tegenfeldt, R.H. Austin, E. Chen, W. Wu, S.Y. Chou, "Fabrication of 10 nm enclosed nanofluidic channels," *Appl. Phys. Lett.*, vol. 81, pp. 174-176, 2002.
[9] J. Gu, R. Gupta, C.F. Chou, Q.H. Wei, F. Zenhausern, "A simple polysilsesquioxane sealing of nanofluidic channels below 10 nm at room temperature," *Lab Chip*, vol. 7, pp. 1198-1201, 2007.
[10] C. Song, P. Wang, "Fabrication of sub-10 nm planar nanofluidic channels through native oxide etch and anodic wafer bonding," *IEEE Trans. Nanotechnology*, vol. 9, pp. 138-141, 2010.
[11] F. Kremer, A. Schönhals, *Broadband dielectric spectroscopy*, 1st ed., Springer, New York, 2003.
[12] G.R. Facer, D.A. Notterman, L.L. Sohn, "Dielectric spectroscopy for bioanalysis: From 40 Hz to 26.5 GHz in a microfabricated wave guide," *Appl. Phys. Lett.,* vol. 78, pp. 996-998, 2001.
[13] S. Mashimo, N. Miura, "High-order and local-structure of water determined by microwave dielectric study," *J. Chem. Phys*., vol. 99, pp. 9874-9881, 1993.
[14] H. Jansson, J. Swenson, "Dynamics of water in molecular sieves by dielectric spectroscopy," *Eur. Phys. J. E*, vol. 12, pp. S51-S54, 2003.
[15] D.M. Pozar, *Microwave Engineering*, 3rd ed., John Wilwy & Sons, Inc, New York, 2005.

978-1-4673-2141-9/13/$31.00 ©2013 IEEE

[16] U. Gösele, Q.Y. Tong, A. Schumacher, G. Krauter, M. Reiche, A. Plossl, P. Kopperschmidt, T.H. Lee, W.J. Kim, “Wafer bonding for microsystems technologies,” *Sens. Actuator A-Phys.,* vol. 74, pp. 161-168, 1999.
[17] R.B. Schoch, H. van Lintel, P. Renaud, “Effect of the surface charge on ion transport through nanoslits,” *Phys. Fluids*, vol. 17, pp. 100601-100605, 2005.
[18] L.J. Cheng, L.J. Guo, “Rectified ion transport through concentration gradient in homogeneous silica nanochannels,” *Nano Letters*, vol. 7, pp. 3165-3171, 2007.
[19] R. Karnik, R. Fan, M. Yue, D.Y. Li, P.D. Yang, A. Majumdar, “Electrostatic control of ions and molecules in nanofluidic transistors,” *Nano Letters*, vol. 5, pp. 943-948, 2005.

978-1-4673-2141-9/13/$31.00 ©2013 IEEE